Kinetics of the Early Stage of Dispersion Polymerization in Supercritical CO_2 As Monitored by Turbidimetry. 2. Particle Formation and Locus of Polymerization

Ulrich Fehrenbacher† and Matthias Ballauff*

Polymer-Institut, Universität Karlsruhe, Kaiserstr. 12, 76128 Karlsruhe, Germany

Received November 13, 2001; Revised Manuscript Received January 25, 2002

ABSTRACT: We present a study of dispersion polymerization of methyl methacrylate in supercritical CO_2 (sc-CO_2) at 330 bar in situ by turbidimetry. All experiments have been done in the presence of the macromonomer poly(dimethylsiloxane)−monomethacrylate (PDMS−MA) which acts as a stabilizer. The formation of particles of poly(methyl methacrylate) (PMMA) can be monitored quantitatively by turbidimetry because the degree of swelling by sc-CO_2 as well as the refractive index of these particles is known accurately. The turbidity spectra were measured in the range 400−950 nm. The number density N/V and the diameter σ_τ could be obtained as a function of time in the earliest stage of the dispersion polymerization with a time resolution of ca. 0.1 s. Moreover, the mass of polymer $m_p(t)$ could be deduced by means of which a full kinetic analysis could be performed. Special attention has been paid to the size distribution of particles that is shown to play an essential role in the treatment of turbidimetric data. It is demonstrated that the locus of polymerization in the early stage studied here is the homogeneous phase. $N/V(t)$ raises quickly in the nucleation period (stage I) and remains then constant (stage II). The diameter of the critical nuclei, i.e., σ_τ, measured in stage I is ca. 150−170 nm. All data obtained are in semiquantitative agreement with the model proposed by Paine.

Introduction

Typical vinyl polymers are only scarcely soluble in supercritical carbon dioxide (sc-CO_2) whereas vinyl monomers mix easily with this solvent.[1] Hence, the polymerization of vinyl monomers, e.g., methyl methacrylate (MMA), in sc-CO_2 proceeds via a dispersion polymerization. Recent work has demonstrated that the dispersion polymerization of MMA in sc-CO_2 leads to well-defined particles with narrow size distribution if suitable surfactants or macromonomers are added.[2−7] This allows to generate polymer particles in an environmentally friendly solvent for a wide range of applications. A systematic application of dispersion polymerization of vinyl monomers in sc-CO_2, however, requires an advanced understanding of the kinetics of this process and its dependence on a large number of variables as for example the concentrations of the monomer, of the initiator, and of the surfactant.

Central to this problem is the very early stage of dispersion polymerization in which the formation of particles takes place. Up to now, the mechanism of particle formation in dispersion polymerization is less well-understood than in emulsion polymerization.[8] According to the model proposed by Paine some years ago, dispersion polymerization proceeds through two stages: (1) a very short nucleation stage in which the primary particles are formed through coagulation and (2) a growth phase in which the number of particles per volume N/V stays constant.[9] In the latter stage, the surfactant covers the particles so that sufficient steric stabilization[7] prevents further coagulation.

The experimental test of the predictions of Paine[9] is faced with considerable difficulties because the first stage of dispersion polymerization is very short. Moreover, the resulting N/V is expected to be small. Electron microscopy is well-suited to study the final particles and to deduce their in-situ diameter if the uptake of sc-CO_2 of the particles is known with sufficient precision. The very early stage cannot be studied by this method (cf. the discussion of this problem by Li et al.[6]). In principle, static and dynamic light scattering is suited to investigate the growth of particles but is soon disturbed by multiple scattering.[10,11] Turbidimetric measurements allow to circumvent this problem because the measured turbidity is insensitive toward multiple scattering and hence suitable for the study of strongly scattering suspensions.[12] Johnston and co-workers[3,4,6] monitored N/V as well the particles diameter σ in the course of the dispersion polymerization of MMA in sc-CO_2. The measurement of the extinction was achieved through pumping the reaction mixture through a separate cell. In this way the length of the optical path could be optimized to allow the measurement of particles up to the range of 1 μm. The experimental setup, however, makes the study of the very early stage of particle formation difficult because of the minimum time needed for cycling the content of the optical cell.

In principle, turbidimetry is the method of choice to follow the growth of particles out of a homogeneous medium. If the total scattering cross section of the sample is measured at several wavelengths, the particle diameter σ and the number density N/V can be determined simultaneously by application of Mie's theory.[12] The practical implementation of this method to the problem at hand, however, is faced with two major difficulties: (i) the refractive indices of the particles of the surrounding medium and its dependence on the wavelength must be known with good accuracy, and (ii) the measured turbidity yields the "turbidity-average" diameter that depends sensitively on the size distribution of the particles.[12−15] Problem (i) is aggravated

† Present address: Fraunhofer Institut Chemische Technologie, Joseph-von-Fraunhofer-Str. 7, 76327 Pfinztal.

* To whom correspondence should be addressed: e-mail Matthias.Ballauff@chemie.uni-karlsruhe.de.

10.1021/ma011985n CCC: $22.00
Published on Web 03/22/2002

by the fact that usual vinyl polymers are swollen by sc-CO_2 considerably which must be taken into account.

In a recent paper we have reported on an investigation of the dispersion polymerization of MMA in the presence of the macromonomer poly(dimethylsiloxane)−monomethyl acrylate (PDMS−MA).[16] This system has already been studied by Johnston and co-workers.[3,4] In our investigation, however, the extinction is measured directly in the reactor, and a long optical path (4.97 cm) allows to monitor small extinctions. Hence, the experimental setup is uniquely suited to detect rather small particles and to look into a very early stage of the dispersion polymerization.

Here we wish to present the continuation of this study conducted on the system MMA/PDMS−MA. The previous analysis[16] is refined by taking into account the difficulties mentioned above. Problem (i) has recently be solved by direct measurements of the refractive indices of the particles n_p and the medium n_0 by waveguide spectroscopy.[17] These measurements gave the degree of swelling of PMMA at the same time. Hence, the refractive index of PMMA particles in sc-CO_2 is now available, and no mixing rules need to be assumed. Problem (ii) is solved by measuring the size distribution in a rather early stage through stopping the reaction and analyzing the particles. Since the turbidity τ has been measured at different wavelengths, the combination of turbidimetry and electron microscopy leads to the determination of the particle size distribution with sufficient accuracy.

It thus becomes possible to determine the size of the particles as well as their number density simultaneously. These data can be used for an analysis of the formation of particles. Since the combination of these parameters gives the mass of the polymer formed at a given time, the kinetics of the dispersion polymerization can be investigated at the same time. Hence, kinetic constants become available from turbidimetric data, and the dispersion polymerization studied here can compared to the bulk polymerization of the same monomer.

Having improved the method of analysis, two major questions that remained open in previous investigations can be tackled: (1) Is there a distinct transition from a nucleation stage to a growth stage in which N/V remains constant? (2) Is the homogeneous phase the locus of polymerization,[16] or does the polymerization take place within the particles? The data obtained here hence can directly compared to the predictions of Paine's model[9] and may therefore be of general significance in the field of dispersion polymerization.

Analysis of Particles Formation by Turbidimetry

The turbidity τ is the attenuation of the beam of light according to $\tau = (1/l)\ln(I_0/I)$, where l is the length of the optical path and I_0 and I are the intensities of the incident and the transmitted light, respectively. If absorption can be excluded, the turbidity is solely due to the scattering of the light by the particles. Hence, τ is related to the intensity of the scattered light by[12,13]

$$\tau = 2\pi\int_0^\pi R(q)\sin\theta\,\mathrm{d}\theta \qquad (1)$$

where $R(q)$ is the Rayleigh ratio for unpolarized light and q is the magnitude of the scattering vector ($q = (4\pi n_0/\lambda_0)\sin(\theta/2)$; λ_0 = wavelength of the incident radiation, n_0 = refractive index of the medium, θ = scattering angle).[13] It is expedient to render the turbidity τ of a suspension of monodisperse particles with diameter σ as the product of an integrated form part $Q(\sigma,\lambda^2,m)$ and an integrated structure factor $Z(\lambda^2,\phi,m)$.[14,15] Hence,

$$\tau = \frac{2\pi}{3}\frac{N}{V}\left(\frac{n_0\pi}{\lambda_0}\right)^4\left(\frac{m^2-1}{m^2+2}\right)^2\sigma^6 Q(\sigma,\lambda^2,m)\,Z(\lambda^2,\phi,m) \qquad (2)$$

where $m = n_p/n_0$ is the relative refractive index of the particles, n_0 is the refractive index of the medium, and N/V denotes the number of particles per unit volume. The volume fraction ϕ of the particles in the system follows as by $\phi = (N/V)(\pi/6)\sigma^3$. Hence, eq 2 shows that τ is dependent on λ through the classical Rayleigh factor λ^{-4} and through $Q(\sigma,\lambda^2,m)$. The integrated form factor $Q(\sigma,\lambda^2,m)$ is normalized to unity for infinite wavelength and can be calculated within the frame of the Mie theory.[14,15] The function $Z(\lambda^2,\phi,m)$ is related to the interaction of the particles and is unity in good approximation for the small volume fraction of particles under consideration here.[16]

The turbidity τ_0 of a system of noninteracting spheres polydisperse sphere follows as[12,15]

$$\tau_0 = \frac{2\pi}{3}\frac{N_{av}}{V}\left(\frac{n_0\pi}{\lambda_0}\right)^4\left(\frac{m^2-1}{m^2+2}\right)^2\sigma_\tau^{\,6}Q_M(\sigma_\tau,\lambda^2,m) \qquad (3)$$

where the measured normalized cross section $Q_M(\sigma_\tau,\lambda^2,m)$ is defined through

$$Q_M(\sigma_\tau,\lambda^2,m) = \sum_i^p \frac{N_i}{V}\sigma_i^{\,6}Q_i(\sigma_i,\lambda^2,m)/\sum_i^p \frac{N_i}{V}\sigma_i^{\,6} \qquad (4)$$

and the turbidity-average diameter σ_τ by[15]

$$\sigma_\tau^{\,3} = \frac{\sum_i^p \frac{N_i}{V}\sigma_i^{\,6}}{\sum_i^p \frac{N_i}{V}\sigma_i^{\,3}} \qquad (5)$$

Given these definitions, the average number density N_{av}/V determined by the turbidimetric analysis follows as

$$\frac{N_{av}}{V} = \frac{\tau_0}{\frac{2\pi}{3}\left(\frac{n_0\pi}{\lambda_0}\right)^4\left(\frac{m^2-1}{m^2+2}\right)^2\sigma_\tau^{\,6}Q_M(\sigma_\tau,\lambda^2,m)} \qquad (6)$$

$Q(\sigma,\lambda^2,m)$ depends strongly on λ if σ_τ is not too small. So both N_{av}/V and σ_τ can be obtained if τ is measured at two wavelengths. The measurements must therefore be done simultaneously at several wavelengths in order to obtain secure results together with appropriate error bars.

The evaluation of data proceeds as follows: τ is determined as the function of t for a sufficient number of wavelengths in the visible range. Then the experi-

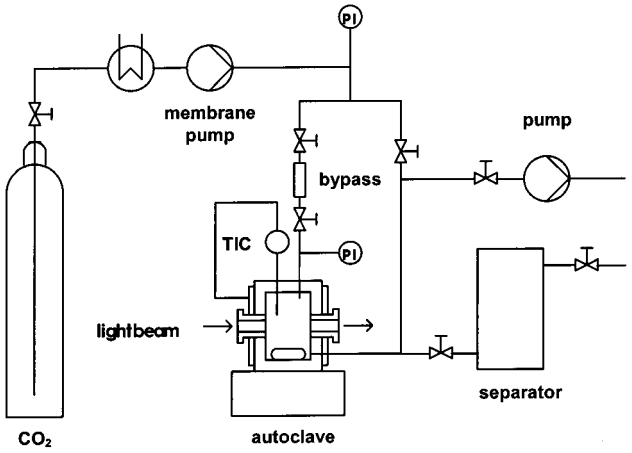

Figure 1. Scheme of the apparatus used for the study of the dispersion polymerization of MMA in sc-CO_2. The polymerization in the autoclave is directly monitored through the measurement of the turbidity. The initiator AIBN is injected through a bypass which starts the reaction. The reaction can be quenched through injection into the separator under pressure. The separator is filled with *n*-octane containing a small amount of methylhydroquinone to stop the radical polymerization. The autoclave is thermostated to ±1 deg.

mental ratio of $\tau_0(\lambda_1)/\tau_0(\lambda_2)$ is compared to values calculated according to

$$\frac{\tau_0(\lambda_1)}{\tau_0(\lambda_2)} = \frac{\left(\frac{m_1^2-1}{m_1^2+2}\right)^2 \left(\frac{n_0(\lambda_1)}{\lambda_1}\right)^4}{\left(\frac{m_2^2-1}{m_2^2+2}\right)^2 \left(\frac{n_0(\lambda_2)}{\lambda_2}\right)^4} \frac{Q_M(\sigma_\tau,\lambda^2{}_1,m_1)}{Q_M(\sigma_\tau,\lambda^2{}_2,m_2)} \quad (7)$$

The dispersion of both the relative refractive index m of the particles as well as of the solvent $n_0(\lambda)$ must be known with sufficient accuracy (cf. Experimental Section). The average diameter σ_τ is varied until the calculated $\tau_0(\lambda_1)/\tau_0(\lambda_2)$ agrees with the experimental data. This calculation that proceeds through eq 4 requires the size distribution $N(\sigma_i)$ as input (see eq 3). Repeating this calculation for several pairs of wavelengths then leads to a consistency check. The correct σ_τ is in turn used to determine N_{av}/V by use of eq 6.

In principle, application of this procedure to sufficiently accurate data would lead to the entire size distribution as well. The problem is ill-posed, however, and only the breadth of the distribution can be determined from turbidimetric data. Therefore, the form of the distribution is deduced from electron microscopy in the course of the present analysis.

Experimental Section

Materials. Methyl methacrylate (MMA; obtained from the Röhm AG) was destabilized by washing with 10 wt % aqueous NaOH and subsequently with water. After careful drying the monomer was distilled in vacuo two times shortly before use. Poly(dimethylsiloxane)−monomethyl acrylate (PDMS−mMA; Aldrich) was used as received. Its weight-average molecular weight was found to $M_w = 14\,000$ g/mol whereas its polydispersity was found to $M_w/M_n = 1.1$ (analyzed against poly(styrene) standards[16]). 2,2′-Azobis(isobutyronitrile) (AIBN, Fluka, analytical grade) was recrystallized in methanol, and CO_2 (grade 5.2; less than 1 ppm of O_2; received from Aga AG) were used without further purification.

Methods. The apparatus used here is shown schematically in Figure 1 and has been described in detail previously.[16] The main component is the autoclave (100 mL) with two sapphire windows. The content of the autoclave can be stirred by a magnetic stirring bar which lies underneath the optical path. The turbidity can be measured directly through these windows (length of the optical path: 4.97 cm) by connecting the cell with light guides to a Zeiss MCS 522 UV/vis/NIR diode array spectrometer in a spectral range of 400−950 nm.

The autoclave is thermostated with the temperature control being better than ±1 °C. Carbon dioxide can be filled into the autoclave under pressure by use of a membrane pump (Lewa, Leonberg, Germany). The apparatus can be evacuated by a vacuum pump, and a bypass allows to inject small amounts of initiator into the pressurized autoclave. The content of the autoclave can be transferred under a pressure into a separator filled with organic solvents (*n*-octane). Thus, the reaction can be quenched and the particles analyzed by electron microscopy.

The size of the particles was determined ex-situ by using a LEO Gemini F2-4 scanning electron microscope (SEM). All samples have been covered by a layer of ca. 10 nm of platinum. Evaluation of data was done using a Zeiss TG3 particle size analyzer.

Experimental Procedure. Prior to each experiment the autoclave was carefully purified from traces of oxygen by heating in vacuo. In a typical run, 10 g of MMA and 0.65 g of PDMS−mMA were filled in under an atmosphere of CO_2. CO_2 was pumped into the autoclave at a temperature until a pressure of 280 bar had been reached. 50 mg of AIBN was filled into the bypass (see Figure 1), which subsequently has been evacuated and filled with CO_2. The pressure of CO_2 in the bypass was higher by approximately 70 bar.

The experiment was started by injecting AIBN with liquid CO_2 under pressure into the autoclave. The injection took place in less than 2 s. After the injection of AIBN the pressure raised to the final pressure of 330 bar. The stirring was continued during the entire experiment. Varying the speed of the stirrer in separate experiments ensured that the stirring had no measurable influence on the kinetics of the early stage of the reaction as expected. The reaction started immediately if the autoclave had been carefully cleansed before the measurements. Traces of oxygen, however, lead to induction periods in excess of a minute.

The extinction was measured simultaneously in the entire spectral range of the spectrometer (400−950 nm). Depending on wavelength (see eq 2), the turbidity increased more or less strongly with time. Only turbidity spectra between $\tau = 0.02$ and 1 cm^{-1} and between 400 and 800 nm were taken for the subsequent evaluation. If τ is smaller, the error is too high, whereas high turbidities are afflicted by forward scattering that is induced by strong multiple scattering.

Quenching of the polymerization could be done by transferring the entire content into the separator filled with *n*-octane under pressure. To stop the radical polymerization immediately, 0.2 wt % hydroquinone had been added to the *n*-octane. The particles resulting from the polymerization in the autoclave were washed carefully with *n*-octane and collected by centrifugation.

The evaluation of the data was done as follows: n_0 was determined by waveguide spectroscopy, and the dispersion of n_0 was deduced from literature data related to different wavelengths and taken at 50 °C.[17,18] The data were fitted by the equation

$$n_0^2 = a + b\lambda^{-2} + c\lambda^{-4} \quad (8)$$

with $a = 1.4773$, $b = 2881.5$ nm^2, $c = -1858.2$ nm,[4] and λ in nm.

An important improvement of the turbidimetric analysis could be achieved through introduction of precise optical data and swelling rates of the particles that have been determined independently by waveguide spectroscopy.[17] Moreover, the refractive index of a PMMA film that had been swollen by an appropriate mixture of MMA and CO_2 could be measured directly. Typical degrees of swelling of the particles are between 27 vol % (pure CO_2, 330 bar) and 40 vol % (1.5 M MMA, CO_2, 330 bar).[17]

The dispersion of the refractive index n_p of the swollen particles could not deduced directly from waveguide spectroscopy because these measurements were done at a given wavelength. Here the following procedure was adopted: A sample polymerized to a degree of conversion of ca. 0.1% was quenched and the size distribution measured by electron microscopy. The turbidity spectra taken just before quenching was used to determine n_p and n_0 as a function of λ by a comparison of the measured and the calculated spectra.[15] As in ref 16, the internal consistency of the turbidimetric analysis could be checked by comparing the results to the diameter taken from electron microscopy.

The molecular weight of the resulting PMMA was determined using a Waters 150-CV GPC with tetrahydrofuran (30 °C) calibrated by poly(styrene) standards ($M_w = 100-7 \times 10^7$ mol/g, PSS, Mainz Germany) and the universal calibration for PMMA.

Results and Discussion

Analysis of τ and Size Distribution. The data reported herein derive from the study of the dispersion polymerization of MMA in the presence of PDMS−MA. To achieve a kinetic analysis of this polymerization, the monomer concentration (0.65−2.2 mol/L), the amount of initiator AIBN (25−180 mg in 100 mL), the macromonomer concentration 6.5 wt % (based on the amount of MMA), and the temperature (55−70 °C) were varied. Given the moderate solubility of the stabilizer PDMS−MA,[3] a pressure of 330 bar was maintained throughout all experiments reported here. A smaller pressure resulted in flocculation at low conversion and poor reproducibility. This observation agrees with similar findings of O'Neill et al.[3,4]

The polymerization was started through injection of AIBN (cf. the description of Figure 1). The onset of particle formation could be seen by a evolving yellowish and then a reddish color. The UV spectrometer used here could take simultaneous measurements at a broad range of wavelengths (400 nm $\leq \lambda \leq$ 950 nm) with excellent accuracy and resolution of time (less than 0.1 s). As already discussed previously, the analysis of τ performed here requires σ_τ to be large enough to render $Q_M(\sigma_\tau,\lambda^2,m)$ dependent on wavelength. This is case for particles with diameters of 80 nm and greater. For smaller particles $Q_M(\sigma_\tau,\lambda^2,m) \approx 1$, and the above analysis for σ_τ and N_{av}/V becomes insecure. The following discussion will show, however, that this restriction does not impede the analysis of the early stage of particle formation. Full conversion is reached only after ca. 500 min, but the analysis done here is restricted to 300 s at the most. The much larger particles formed after longer reaction time are difficult to measure because of their strong forward scattering[13] that would render the obtained turbidities less accurate.[15]

The analysis of the turbidity τ between $\lambda = 500-800$ nm for σ_τ and N_{av}/V rests on the accurate determination of the size distribution that has been derived from electron microscopy. Figure 2 displays typical results from such an analysis obtained by quenching after 340 s. Here Figure 2a shows the micrograph whereas Figure 2b displays the resulting size distribution taken therefrom. Special care has been taken to take into account only particles located directly at the surface (see Figure 2a). At least 680 particles from several micrographs were thus used for the determination of the size distribution. It need to be noted that the analysis by of the size distribution could not be done at a very early stage because the number of particles was too small in this regime.

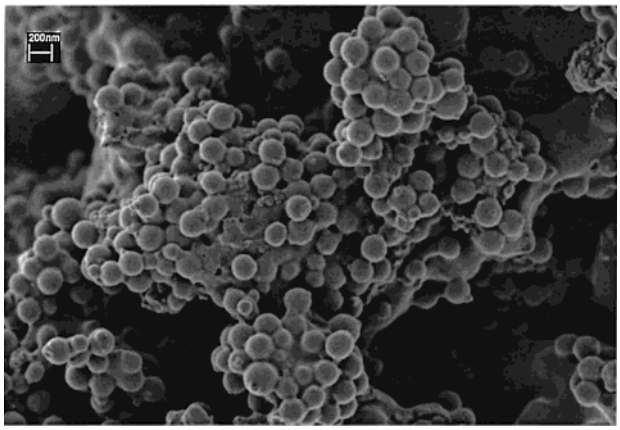

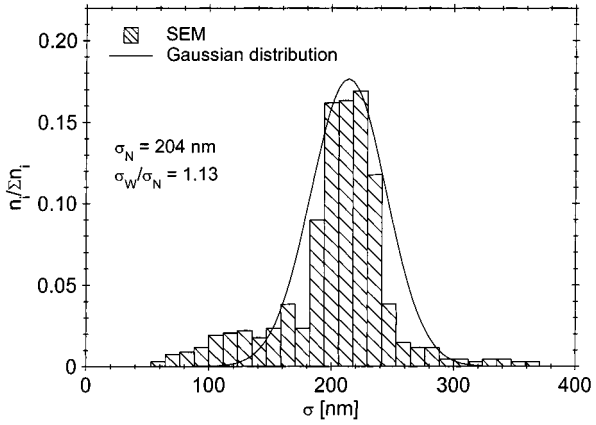

Figure 2. Analysis of the size distribution by electron microscopy. (a) Micrograph obtained by scanning electron microscopy taken after 340 s. (b) Number distribution that resulted from counting 680 particles. The line gives the best fit of the distribution by a Gaussian. Monomer concentration = 0.95 mol/L; concentration of PDMS−MA = 6.5 wt % relative to MMA; amount of AIBN = 49.9 mg (0.003 mol/L).

Evidently, the experimental distribution cannot be well described by a Gaussian but is skewed toward smaller particles. The polydispersity is rather small, however, and the electron micrograph demonstrates directly the fact that well-defined particles are obtained under the experimental conditions applied here.

Figure 3 displays a typical set of data resulting from this analysis. Here σ_τ and N_{av}/V are plotted as a function of reaction time t together with the respective error bars. As already discussed above, the turbidimetric analysis becomes more secure with increasing particles size. It is evident, however, that both quantities can be determined after $t > 40$ s. Moreover, the dependence of N_{av}/V on time demonstrates that the dispersion polymerization of the present systems proceeds through two stages indeed: The average number of particles first increases markedly (stage I) and stays practically constant in a second stage ($t > 150$ s). At the same time the average diameter σ_τ of the particles is at first virtually constant but increases in a monotonic fashion at longer times.

It must be kept in mind that the turbidimetric analysis resulting in σ_τ and N_{av}/V is very sensitive toward a change of the size distribution. A small decrease of N_{av}/V after longer times may well reflect a narrowing of the distribution that escapes the analysis by REM as applied here. Concomitantly, σ_τ may become slightly too large by this effect. Since the size distribution is determined mostly in a later stage of the

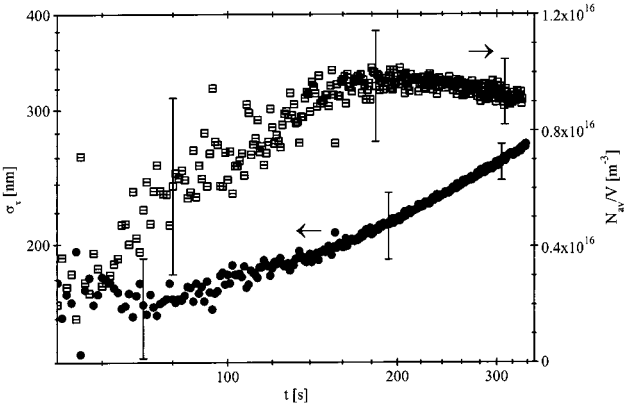

Figure 3. Turbidity-average diameter σ_τ and average number density N_{av}/V of the particles as a function of time (monomer concentration = 0.95 mol/L; concentration of PDMS−MA = 6.5 wt % relative to MMA; amount of AIBN = 49.9 mg (0.003 mol/L); temperature = 60 °C) together with the respective error bars. The calculation of the data has been done using the experimental particle distribution (cf. the discussion of Figure 2). The larger error at shorter times is due to the smaller size of the particles that is followed by $Q_M(\sigma_\tau,\lambda^2,m) \approx 1$ and a less secure evaluation of the data according to eq 7.

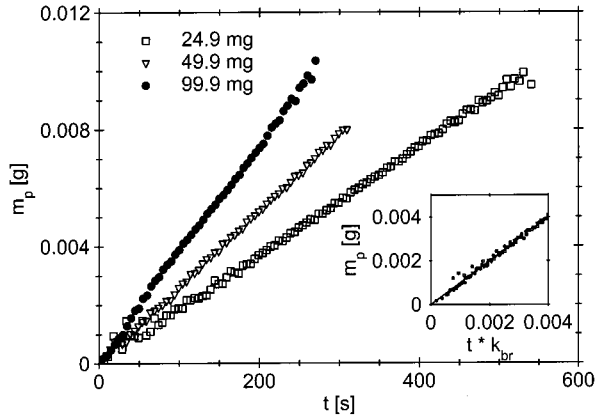

Figure 4. Mass m_p of PMMA as a function of reaction time t. Parameter of the different curves is the amount of added initiator AIBN indicated in the graph. The concentration of MMA was 0.95 mol/L, the concentration of PDMS−MA was 6.5 wt % relative to MMA, and the temperature was 60 °C. The inset shows the same data but as a function of t scaled by the rate constant k_{br} that has been take from the slope of the curves.

polymerization, the data of σ_τ and N_{av}/V deriving shortly before quenching are of highest accuracy and will be taken for further evaluations. In view of the error bars in Figure 3, the slight decrease of N_{av}/V will not be considered in detail.

Overall Kinetics and Locus of Polymerization. The product of σ_τ^3 and N_{av}/V thus determined then may be used to calculate the total amount m_p of polymer formed at time t.[16] The degree of swelling of the particles by the mixture of CO_2 and MMA determined in ref 17 has been used for this calculation. The density of the PMMA was calculated from literature data.[19] This calculation is admissible because PMMA of the molecular weight formed here is totally insoluble in sc-CO_2 under the conditions employed here.[17] In this way turbidimetry serves as a microbalance that allows to weight minute amounts of polymer and hence to perform a conventional kinetic analysis. Figure 4 displays a set of data obtained at different initiator concentrations. Parameter of the different curves is the amount of added initiator AIBN. The strictly linear increase of m_p as a function of t is directly evident, and the slope of these curves may be converted to the respective rate constants k_{br}. The inset of Figure 4 proves the consistency of this procedure. All data collapse to a single master curve if t is scaled by the slope k_{br} of the curves. The determination of the entire amount m_p is afflicted by a considerably smaller error than is the case the evaluation of σ_τ and N_{av}/V. Turbidimetry is mainly sensitive to the total cross section of the sample, i.e., the entire amount of polymer converted to particles. The decomposition into σ_τ and N_{av}/V, however, requires evaluation of a more subtle effect, namely the dependence of τ on wavelength.

As already discussed previously,[16] there a short induction period of 10−50 s which has been subtracted from t in all data to be discussed here. It must be noted that this short induction time is only obtained if the autoclave is carefully heated under CO_2 prior to the experiments; otherwise, much longer induction periods result. Small amounts of impurities sticking to the wall of the container that might disturb the polymerization must hence be removed.

The data shown here demonstrate that the rate of the polymerization stays constant within the stage analyzed here. No acceleration or other changes of R_p take place. Thus, the radical polymerization can be analyzed in the usual manner.[20] Moreover, the data show that the present study is restricted to exceedingly low conversions. Hence, all parameters stay virtually constant, and no change of the monomer concentration or of other educts must be taken into account.

The rates R_p of polymerization obtained for different amounts of AIBN are displayed in Figure 5a whereas Figure 5b gives the respective result for the variation of the monomer concentration. Figure 5c shows the dependence of the rate constant on temperature for a given set of parameters (330 bar, 0.6−2.2 mol/L MMA, 0.003 mol/L AIBN, 0.65 wt % PDMS−MA).

The data demonstrate that the overall kinetics of the dispersion polymerization in the early stage exhibits the usual dependencies, namely,

$$R_p = k_{app}[M][AIBN]^{0.5} \qquad (9)$$

The rate constant exhibits the expected dependence on temperature (activation energy: 72 kJ/mol). Moreover, the measured apparent rate constant k_{app} (=5×10^{-5} mol$^{-1/2}$ L$^{1/2}$ s^{-1}; T = 60 °C, 330 bar) is in good agreement with independent estimates. For this calculation, the decay constant k_d of AIBN and the efficiency f in sc-CO_2 furnished by DeSimone et al. were used ($k_d = 3.5 \times 10^{-6}$ s^{-1}; f = 0.83).[21] The termination constant k_t of PMMA radials in sc-CO_2 is higher by 1 order of magnitude as compared to polymerization in solution.[22,23] Here we used the value $k_t \approx 10^8$ s^{-1}.[22] The propagation constant k_p was taken from literature.[24,25] It decreases to 60% of its value in bulk polymerization.[26]

Thus, k_p = 623 L mol^{-1} s^{-1} has been used for the present estimate. With these data and assumptions the apparent rate constant $k_{app} \approx 1 \times 10^{-4}$ mol$^{-1/2}$ L$^{1/2}$ s^{-1} whereas the experimental value is 5×10^{-5} mol$^{-1/2}$ L$^{1/2}$ s^{-1}. Given the various sources of error this may be regarded as satisfactory agreement. The molecular weight calculated[20] from the above constant

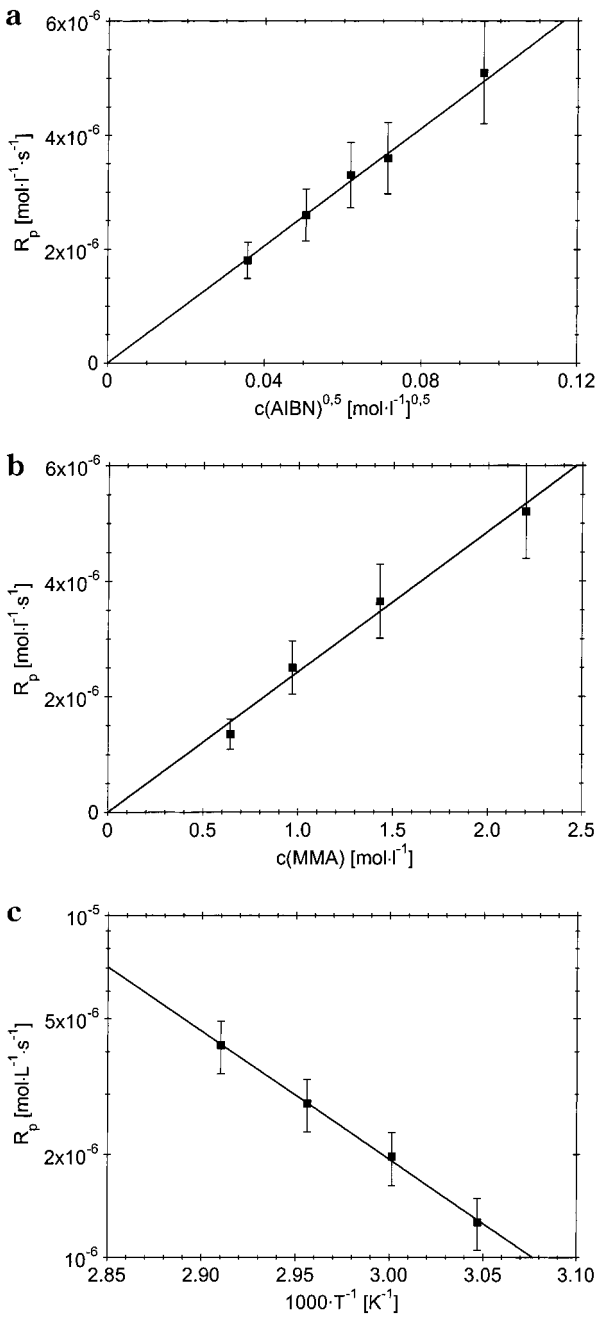

Figure 5. Analysis of the overall kinetics of the dispersion polymerization. (a) Rate R_p of polymerization as the function of the concentration of the initiator AIBN. The concentration of MMA was 0.95 mol/L, the concentration of PDMS−MA was 6.5 wt % relative to MMA, and the temperature was 60 °C. (b) Rate R_p of polymerization as a function of monomer concentration. The concentration of AIBN was 0.003 mol/L, the concentration of PDMS−MA was 6.5 wt % relative to MMA, and the temperature was 60 °C. (c) Rate R_p of polymerization as the function of temperature. The concentration of monomer was 0.95 mol/L, AIBN was 0.003 mol/L, and the concentration of PDMS−MA was 6.5 wt % relative to MMA.

results to 33 000 g/mol whereas the experimental value (taken from the quenched PMMA particles) was 40 000 g/mol.

This demonstrates that the dispersion polymerization of MMA must be confined to the continuos phase in this stage. This can also be argued from the fact that a polymerization solely in the particles would proceed much slower.[16] This case is described by the well-known case 2 of the Smith−Ewart theory, and R_p should be given by[20]

$$R_p = \frac{1}{2} k_p [M] \frac{N_{av}}{V} \tag{10}$$

where [M] is the monomer concentration in the swollen PMMA particles. Given the data for the present conditions (T = 60 °C, [AIBN] = 0.003 mol/L, [MMA] = 0.95 mol/L, and $R_p = 2.5 \times 10^{-6}$ mol L^{-1} s^{-1}), the resulting rate R_p is estimated to be smaller by 3 orders of magnitude. This is mainly due to the rather small number density of particles as compared to conventional emulsion polymerization. Evidently, polymerization within the particles plays no role in the early stage of the dispersion polymerization studied here.

The present results demonstrate unambiguously that the polymerization takes place in the continuous phase. Polymerization within the particles can play no significant role. Hence, the particles can only grow through precipitation of polymer onto their surface. If growing radicals are adsorbed onto a particle, the polymerization may go on for some time, but this process cannot contribute significantly to the observed rate. It must be reiterated that the present experimental setup only looks into the early stage of dispersion polymerization. In a later stage where much larger particles are present and where the concentration of monomer in the homogeneous phase has decreases considerably, polymerization can take place within the particles.[27]

Particle Formation. Having clarified the kinetics of polymerization, the formation of particles will be discussed next in terms of N_{av}/V and σ_τ. It is expedient to discuss first the dependence of these quantities on the concentration of initiator. The discussion of Figure 3 had already demonstrated that the dispersion polymerization studied here proceeds through two stages: At first N_{av}/V grows approximately linear to reach a critical value $(N_{av}/V)_{crit}$ but stays virtually constant in the second stage. If a distinct mechanism of particle formation is present, the evolution of N_{av}/V and $(N_{av}/V)_{crit}$ should only depend on the amount of polymer formed in the continuous phase. The concentration of the initiator only changes the rate of polymerization but no other variable of the system. This is in opposite to the monomer concentration that influences parameters as for example the swelling of the particles and the precipitation of the copolymer chains. Hence, experiments varying the initiator concentration serve for a sensitive test of this prediction at the end of the turbidimetric measurement in Figure 3.

Figure 6a shows that all data obtained for a given monomer concentration but different initiator concentrations collapse approximately on a master curve if t is scaled with the respective rate constants k_{br}. N_{av}/V as a function of time increases to reach a final value $(N_{av}/V)_{crit}$ that only depends on the amount of polymer formed so far. Moreover, the data demonstrate that stage I in which the particles are formed is restricted to conversions lower than 0.1%. Hence, there is an extremely short time in which the particles are formed but a much longer period in which growth takes places. This is followed by a narrow size distribution of the particles as analyzed by electron microscopy (see the discussion of Figure 2).

The entire mass m_p of polymer together with $(N_{av}/V)_{crit}$ may then serve to calculate $(\sigma_\tau)_{crit}$, the critical

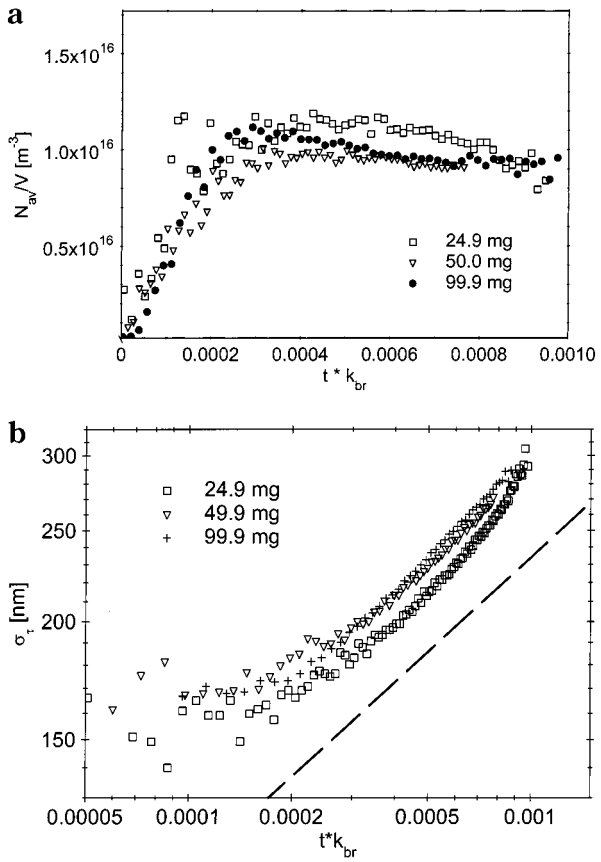

Figure 6. Analysis of the particle formation in the course of dispersion polymerization. Here the dependence on the initiator concentration is shown. The concentration of MMA was 0.95 mol/L, the concentration of PDMS−MA was 6.5 wt % relative to MMA, and the temperature was 60 °C. The amount of the initiator AIBN used in each run is indicated in the graph. The induction period of 10−50 s was subtracted from t in all curves. (a) The average number of particles per volume N_{av}/V is plotted against the reduced reaction time tk_{br}. The plot shows that N_{av}/V depends only on the amount of polymer formed at a given time but not on the concentration of the initiator. (b) The diameter σ_τ is plotted against the reduced reaction time tk_{br}. The dashed line marks the a slope of $^1/_3$. The data demonstrate that σ_τ also depends only on the amount of polymer formed at a given time.

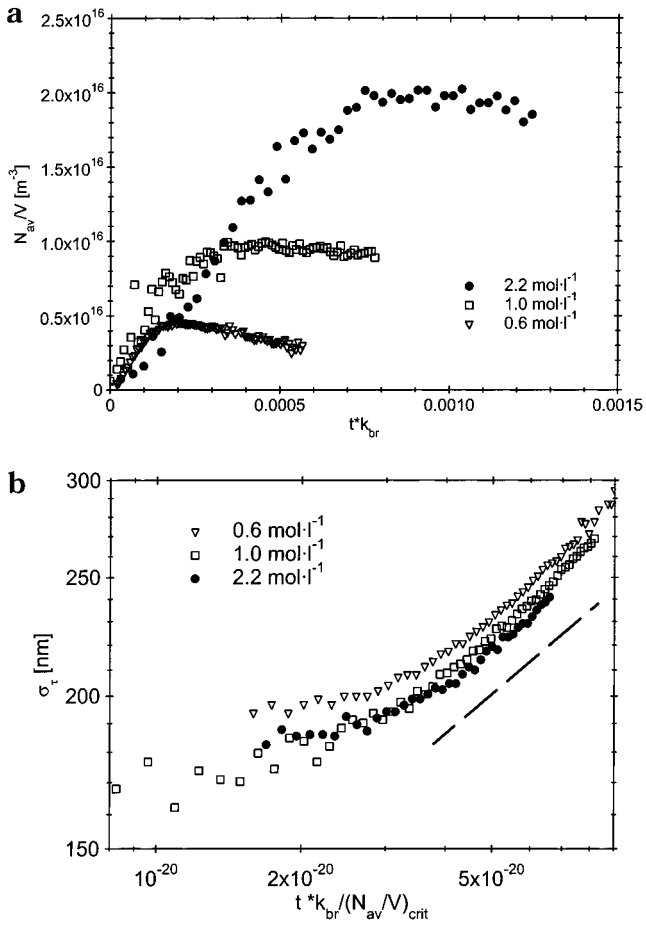

Figure 7. Analysis of the particle formation in the course of dispersion polymerization. Here the dependence on the monomer concentration is shown. The amount of AIBN was 49.9 mg (0.003 M). The concentration of the monomer used in each run is indicated in the graph. (a) The average number of particles per volume N_{av}/V is plotted against the reduced reaction time tk_{br}/C_{MMA}. The two stages of precipitation polymerization are clearly visible: In stage I the particles are formed until a critical number density $(N_{av}/V)_{crit}$ is reached; in the second stage N_{av}/V remains constant. The plot shows that the plateau value $(N_{av}/V)_{crit}$ depends on the concentration of monomer. Within limits of error, however, the rate of formation of new particles, i.e., the slope of these curve in the beginning, is independent of c(monomer). (b) The diameter σ_τ is plotted against the reduced reaction time $tk_{br}/(N_{av}/V)_{crit}$. The reduction of the reaction time thus effected takes into account that the polymer formed at time $k_{br}t$ is precipitated on to $(N_{av}/V)_{crit}$ particles. The critical number density $(N_{av}/V)_{crit}$, on the other hand, is different in each run as shown in (a). (b) demonstrates that the two stages of the precipitation polymerization are clearly visible: A nucleation period in which the particles are formed, and a growth period in which the diameter growths approximately with $t^{1/3}$ whereas N_{av}/V stays constant.

radius of particles. Alternatively, $(\sigma_\tau)_{crit}$ can be taken directly from plots of σ_τ as a function of the reduced time $k_{br}t$. Figure 6b displays σ_τ as a function of time and shows that σ_τ stays approximately constant in stage I but increases with $t^{1/3}$ in stage II where only growth takes place. All data shown in Figure 6b collapse on a master curve within the limits of error. Moreover, Figure 6b shows that $(\sigma_\tau)_{crit}$ is ca. 150−170 nm for the present conditions. The determination of σ_τ is afflicted by a considerably error, in particular at short times, however. But Figure 6a,b demonstrate clearly the consistency of both N_{av}/V and σ_τ as taken from turbidimetry.

Figure 7a displays N_{av}/V as the function of the reduced time $k_{br}t$ obtained for different monomer concentrations. Here the amount of PDMS−MA has been changed concomitantly (6.5 wt % of monomer). The results show that $(N_{av}/V)_{crit}$ now increases on the amount of monomer because the concentration of the stabilizer is increased at the same time. The rate of particle formation is solely related to the rate of formation of polymer. This directly evident from the same slope of $N_{av}/V(k_{br}t)$ in the initial stage in which solely formation of particles takes place.

Since $(N_{av}/V)_{crit}$ differs now in the experiments shown in Figure 7a, the growth of the particles as expressed through the diameter σ_τ as a function of time must now be related to the amount of polymer available per particle. Hence, the reduced time tk_{br} has been divided by the number density $(N_{av}/V)_{crit}$ of the particles reached at the end of the nucleation period. This takes into account that the same amount of polymer formed at time tk_{br} is now precipitating on a different number of particles present in the system. Figure 7b displays the resulting plot. Again the two stages are apparent. All data collapse on a master curve within the given limits

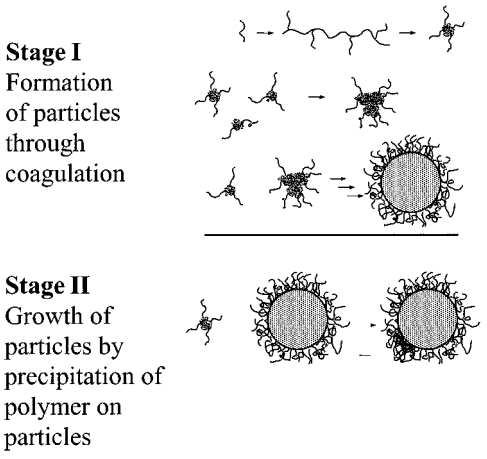

Figure 8. Scheme of the modeling of dispersion polymerization by a two-stage mechanism: At $t = 0$ the monomer and the initiator a fully dissolved in the sc-CO_2. The polymer is formed in the homogeneous phase. Oligomers are still soluble in the solvent, but the solubility decreases rapidly with increasing molecular weight. In stage I the particles are formed through coagulation of polymer that is no longer soluble in sc-CO_2. Hence, new particles are formed, and N_{av}/V increases with time until a critical value $(N_{av}/V)_{crit}$ is reached. In stage II the number of particles N_{av}/V remains constant because all newly formed polymer is precipitated onto the surface of the particles. Therefore, the diameter σ_τ grows as $t^{1/3}$.

of error. This again suggests that $(\sigma_\tau)_{crit}$ is independent of the concentration of monomer, and its value deduced from this set of data is again given by ca. 150−170 nm. Moreover, in stage II all particles grow strictly through precipitation of the polymer generated in the continuous phase; no new particles are formed. Hence, the diameter σ_τ scales approximately with $t^{1/3}$ as expected from previous data (see the discussion of Figure 6b). Therefore, the data displayed in Figure 7 lead to the same conclusion already drawn from Figure 6: The formation of new particles as well as their growth depend directly on the amount of polymer formed as a function of time. The higher N_{av}/V is solely due to the higher amount of stabilizer increased concomitantly with the concentration of monomer.

The model proposed for the formation of particles is displayed in Figure 8. It follows in essence the suggestion of Paine.[9] In stage I particles are formed through coagulation of single polymer chains and instable small particles. The size of these primary particles is rather large (ca. 150−170 nm), and stability is only achieved if the entire surface is covered by PDMS chains. According to Paine's model σ_{crit} is given by eqs 13 and 17 in ref 9

$$\sigma_{crit} = \frac{6[M]M_M Q_{min}}{\rho C_S [S] N_A} \tag{11}$$

where M_M is the molecular weight of the repeating unit, Q_{min} is the minimal coverage of the particles surface by the surfactant, C_S is the ratio of the reactivities of PDMS−MA and MMA, [S] is the concentration of stabilizer, and N_A is Avogadro's number.[9] C_S corresponds the reciprocal copolymerization constant of PDMS−MA and MMA in organic solvents ($C_S = 0.5$).[28] Q_{min} may be estimated by assuming that

$$Q_{min} = \frac{1}{\pi R_g^2} \tag{12}$$

where R_g is the radius of gyration of the CO_2-philic part of the stabilizer. This implies that the minimum surface needed for a stabilizer chain is determined by the "mushroom" conformation[29] of the block that extends into the continuous phase. For R_g was taken a literature value ($R_g = 2.9$ nm).[30]

In a similar manner, Paine's model[9] allows to calculate the final diameter σ_f of the particles and the number density $(N/V)_{crit}$. With the kinetic data discussed above $(N/V)_{crit}$ is predicted to be of the order of $10^{15}-10^{16}$ particles/m^3 (which is found indeed). The final diameter σ_f is typically of the order of 2500 nm whereas the calculated values is ca. 3500 nm. The critical radius of the nuclei $(\sigma_t)_{crit}$ is predicted to be ca. 150 nm: This compares favorably with the present findings, which suggest a value of 150−170 nm. Given the various sources of error in these estimates, the agreement of theory and experiment can be regarded as satisfactory.

Conclusions

The early stage of dispersion polymerization of MMA in sc-CO_2 has been studied by turbidimetry. The average number of particle N_{av}/V, the turbidity-average diameter σ_τ, and the mass of polymer m_p as a function of time have been derived from these data for conversions lower than 0.1%. The mass of PMMA $m_p(t)$ leads to a kinetic analysis of the polymerization whereas N_{av}/V and σ_τ allowed to reveal the different stages of particle formation and growth. In this way the kinetics of polymerization as well as the formation of particles can be studied at the same time. Hence, a full analysis of the dispersion polymerization and a quantitative comparison with theory becomes possible. The analysis leads to the following main conclusions:

(i) In the early stage investigated here the polymerization takes solely place in the homogeneous phase. This can be concluded from the kinetic analysis of the reaction rates and from a comparison of the experimental rates with theoretical estimates.

(ii) The dispersion polymerization proceeds through two stages: In stage I the polymer forms new particles with a critical diameter $(\sigma_\tau)_{crit}$ of 150−170 nm. After this very short period of particle formation all polymer precipitates on the particles. In this second stage N_{av}/V remains constant. The rate of polymerization, however, remains constant in all stages. This again demonstrates that the particles cannot be the locus of polymerization. In the very early stage under investigation here the polymerization takes solely place in the bulk phase.

(iii) The experimental data derived from this analysis are in semiquantitative agreement with the model proposed by Paine.[9] This demonstrates that the steric stabilization by the macromonomer PDMS−MA is the decisive factor that determines the critical diameter $(\sigma_\tau)_{crit}$ of the particles and hence their final size.

Acknowledgment. Financial support by the Deutsche Forschungsgemeinschaft, Schwerpunkt "Überkritische Fluide", is gratefully acknowledged. The authors are indebted to Th. Hirth, Fraunhofer Institut für Chemische Technologie, Pfinztal-Berghausen, Germany, for helpful discussions and technical support.

References and Notes

(1) Kirby, C. F.; McHugh, M. A. *Chem. Rev.* **1999**, *99*, 565.
(2) Kendall, J. L.; Canelas, D. A.; Young, J. L.; DeSimone, J. M. *Chem. Rev.* **1999**, *99*, 543.

(3) O'Neill, M. L.; Yates, M. Z.; Johnston, K. P.; Smith, C. D.; Wilkinson, S. P. *Macromolecules* **1998**, *31*, 2838.
(4) O'Neill, M. L.; Yates, M. Z.; Johnston, K. P.; Smith, C. D.; Wilkinson, S. P. *Macromolecules* **1998**, *31*, 2848.
(5) Christian, P.; Giles, M. R.; Griffiths, R. M. T.; Irvine, D. J.; Major, R. C.; Howdle, S. M. *Macromolecules* **2000**, *33*, 9222.
(6) Li, G.; Yates, M. Z.; Johnston, K. P.; Howdle, S. M. *Macromolecules* **2000**, *33*, 4008.
(7) Johnston, K. P. *Curr. Opin. Colloid Polym. Sci.* **2000**, *5*, 351.
(8) Croucher, M. D.; Winnik, M. A. In Candau, F., Ottewill, R. H., Eds.; *Polymer Colloids*; Kluwer Academic Press: Dordrecht, 1990.
(9) Paine, A. J. *Macromolecules* **1990**, *23*, 3109.
(10) Shen, S.; Sudol, E. D.; El-Aasser, M. S. *J. Polym. Sci., Part A: Polym. Chem.* **1994**, *32*, 1087.
(11) Lacroix-Desmazes, P.; Guyot, A. *Colloid Polym. Sci.* **1996**, *274*, 1129.
(12) Penders, M. H. G. M.; Vrij, A. *J. Chem. Phys.* **1990**, *93*, 3704.
(13) Kerker, M. *The Scattering of Light and Other Electromagnetic Radiation*; Academic Press: New York, 1969.
(14) Apfel, U.; Grunder, R.; Ballauff, M. *Colloid Polym. Sci.* **1994**, *272*, 820.
(15) Apfel, U.; Hörner, K. D.; Ballauff, M. *Langmuir* **1995**, *11*, 3401.
(16) Fehrenbacher, U.; Muth, O.; Hirth, Th.; Ballauff, M. *Macromol. Chem. Phys.* **2000**, *201*, 1532.
(17) Fehrenbacher, U.; Jacob, Th.; Berger, T.; Knoll, W.; Ballauff, M. *Fluid Phase Equilib.*, in press.
(18) Michels, A.; Hamers, J. *Physica* **1937**, *4*, 995.
(19) Hellwege, K.-H.; Knappe, W.; Lehmann, P. *Kolloid Z.* **1962**, *183*, 110.
(20) Odian, G. *Principles of Polymerization*, 3rd ed.; Wiley: New York, 1991.
(21) Guan, Z.; Combes, R. R.; Menecelolu, Y. Z.; DeSimone, J. M. *Macromolecules* **1993**, *26*, 2663.
(22) Beuermann, S. Unpublished measurements.
(23) Beuermann, S.; Buback, M.; Isemer, C.; Wahl, C. *Makromol. Chem. Rapid Commun.* **1999**, *20*, 26.
(24) Beuermann, S.; Buback, M.; Russell, G. T. *Macromol. Chem. Rapid Commun.* **1994**, *15*, 647.
(25) Beuermann, S.; Buback, M.; Davis, T. P.; Gilbert, R. G.; Hutchinson, R. A.; Olaj, O. F.; Russell, G. T.; Schweer, J.; van Herk, A. M. *Macromol. Chem. Phys.* **1997**, *198*, 1545.
(26) Beuermann, S.; Buback, M.; Schmaltz, C.; Kuchta, F. D. *Macromol. Chem. Phys.* **1998**, *199*, 1209.
(27) Lepilleur, C.; Beckmann, E. J. *Macromolecules* **1997**, *30*, 745.
(28) Cameron, G. G.; Chisolm, M. S. *Polymer* **1985**, *26*, 437.
(29) De Gennes, P. G. *Adv. Colloid Interface Polym. Sci.* **1987**, *27*, 189.
(30) Brandrup, J.; Immergut, E. M. *Polymer Handbook*, 3rd ed.; John Wiley & Sons: New York, 1989.

MA011985N